



OPEN ACCESS

EDITED BY

Silvia Capuani,
National Research Council (CNR), Italy

REVIEWED BY

Naoto Yagi,
Japan Synchrotron Radiation Research
Institute, Japan
Juergen Goldschmidt,
Leibniz Institute for Neurobiology (LG),
Germany

*CORRESPONDENCE

Md Motiur Rahman Sagar,
✉ motiur.sagar@mpinat.mpg.de

RECEIVED 16 May 2024

ACCEPTED 13 August 2024

PUBLISHED 26 August 2024

CITATION

Sagar MMR, Svetlove A, D'Amico L,
Pinkert-Leetsch D, Missbach-Guentner J,
Longo E, Tromba G, Bohnenberger H, Alves F
and Dullin C (2024) Optical clearing: an
alternative sample preparation method for
propagation based phase contrast μ CT.
Front. Phys. 12:1433895.
doi: 10.3389/fphy.2024.1433895

COPYRIGHT

© 2024 Sagar, Svetlove, D'Amico, Pinkert-
Leetsch, Missbach-Guentner, Longo, Tromba,
Bohnenberger, Alves and Dullin. This is an
open-access article distributed under the terms
of the [Creative Commons Attribution License
\(CC BY\)](https://creativecommons.org/licenses/by/4.0/). The use, distribution or reproduction in
other forums is permitted, provided the original
author(s) and the copyright owner(s) are
credited and that the original publication in this
journal is cited, in accordance with accepted
academic practice. No use, distribution or
reproduction is permitted which does not
comply with these terms.

Optical clearing: an alternative sample preparation method for propagation based phase contrast μ CT

Md Motiur Rahman Sagar^{1*}, Angelika Svetlove¹,
Lorenzo D'Amico^{2,3}, Diana Pinkert-Leetsch⁴,
Jeannine Missbach-Guentner⁴, Elena Longo², Giuliana Tromba²,
Hanibal Bohnenberger⁵, Frauke Alves^{1,4,6} and
Christian Dullin^{1,2,4,7}

¹Translational Molecular Imaging, Max-Planck-Institute for Multidisciplinary Sciences, Goettingen, Germany, ²Elettra Synchrotron SCpa Trieste, Trieste, Italy, ³Department of Physics, University of Trieste, Trieste, Italy, ⁴Institute for Diagnostic and Interventional Radiology, University Medical Center Goettingen, Goettingen, Germany, ⁵Clinical Pathology, University Medical Center Goettingen, Goettingen, Germany, ⁶Clinic for Haematology and Medical Oncology, University Medical Center Goettingen, Goettingen, Germany, ⁷Diagnostic and Interventional Radiology, University Hospital Heidelberg, Heidelberg, Germany

Synchrotron radiation propagation-based phase-contrast micro-computed tomography (SR μ CT) has been used increasingly for detailed characterization of tissue specimens, alternative to classical histology. It allows rapid and non-destructive three-dimensional (3D) virtual histology of unstained specimens. Although many studies show that standard protocols for formalin-fixation and paraffin-embedded (FFPE) tissue specimens are well suited for propagation based phase-contrast imaging (PBI), refinement of sample preparation protocols for this relatively recent development is still in its early stage. There are several limitations using FFPE blocks including air-bubble inclusion, and crack formation, which affect the quality of the micro-CT scans. In this study we demonstrate that optical clearing of colon cancer specimen followed by embedding in Phytigel, as an alternative sample preparation protocol yields comparable PBI micro-CT image quality and mitigates the aforementioned drawbacks of FFPE specimens. Moreover, since single-distance phase retrieval algorithms for PBI image reconstruction expect scanned materials to be either weakly-absorbing or having a fixed ratio between absorption and phase shift, we hypothesize that optical clearing will result in specimens that are well in line with these mathematical assumption of the applied phase retrieval algorithm (homogeneous form of the Transport-of-Intensity equation TIE-HOM). In addition, we show that classical histological analysis is still possible after re-embedding of the specimen in paraffin. Thus, the proposed novel workflow to scan optical cleared specimens using SR μ CT can be used in combination with light sheet microscopy and can be integrated in a classical pipeline for pathological tissue characterization.

KEYWORDS

optical clearing, BABB, FFPE, synchrotron, x-ray, phase-contrast, micro-CT, virtual histology

1 Introduction

Micro computed tomography (micro-CT) has become a well-established method to study fixed tissue specimens in 3D at cellular resolution - an application often called virtual histology [1–3]. Especially, phase contrast computed tomography with its elevated soft-tissue contrast is often utilized for this purpose as it does not require any additional staining of the tissue and performs well in standard formalin fixed and paraffin embedded (FFPE) tissue [4]. In addition, it has been shown that propagation based imaging (PBI) acquisition does not interfere with subsequent histological analysis [3, 5], allows guiding the histological sectioning process to regions of interest [6] and enables the registration of additional follow-up spatially resolved analysis techniques such as classical histology [7] or atomic force microscopy [8]. Moreover, PBI can be used to supplement studies that deal with 3D structural analysis [9–11] of tissue specimens. Due to these facts, PBI based tissue analysis is becoming more prevalent in biomedical research [12–19].

The principle of PBI is to generate images in which the contrast is predominantly related to phase shifts rather than to x-ray attenuation as used in classical CT. To this end, typically, a so-called phase retrieval algorithm is employed prior to 3D reconstruction. Phase retrieval algorithms rely either on the acquisition of data at multiple sample-to-detector distances [20] or in case of single-distance, on rigorous assumptions regarding the optical properties of the studied specimens. Probably, the most popular algorithm for single distance phase retrieval is the homogeneous form of the Transport-of-Intensity equation (TIE-HOM) [21], which assumes that the studied object is weakly absorbing or has a constant ratio between absorption and phase shift - conditions that in multi-tissue specimens are strictly never fulfilled. As a consequence the parameter of the algorithm can be tuned to generate sharp interfaces only for a specific material combination, leaving other interfaces slightly blurred. This effect has been described by Beltran et al. [22] proposing a combination of multiple phase retrieval steps.

In addition, the quality of the obtained PBI scans highly depends on the method and quality of the sample preparation. While FFPE is doubtlessly the most widely used method for preserving tissue and making it available for subsequent analysis, it has several limitations when used in combination with PBI: a) air bubbles within the embedded tissue or on its surface are often unavoidable leading to strong contrast in PBI; b) the typical high x-ray radiation dose can cause progressive crack formation resulting in motion artifacts in the reconstructed data; and c) the granulated paraffin used in the embedding process of FFPE specimens are prone to become brittle when imaged under a strong x-ray exposure which in turn complicates the subsequent sectioning process for histological analysis. Other embedding materials such as agarose or resin are often not suitable alternatives either. Agarose tends to boil especially at the tissue surface while being scanned under strong x-ray radiation, and due to required re-embedding step of specimens into paraffin, follow-up histological analysis becomes more challenging. This problems of air bubble formation and movement has also been seen in Agar by Strotton et al. [23]. Resin withstands strong irradiation but is

usually not suitable for routine soft-tissue histology due to long embedding time and more complicated cutting procedures [24].

In this study, we compare PBI based virtual histology of human colon cancer biopsies scanned as FFPE tissue blocks with images obtained of the same samples embedded in Phytigel following optical clearing and scanned in the optical clearing solution benzyl alcohol/benzyl benzoate (BABB). Here we show that the SR μ CT of optically cleared colon samples overcomes the aforementioned limitations of using FFPE samples and has similar if not better image quality in single-distance PBI by generating tissue properties well in line with mathematical assumptions of the phase retrieval algorithm.

2 Methods

2.1 Ethics

Human colon carcinoma specimens from different patients were obtained from the Department of Pathology, University Medical Center (Göttingen, Germany) where pathological diagnosis was made as part of each patient's treatment plan. The study was performed according to the guidelines of the local ethics committee of the University Medical Center Göttingen (permission number 24/4/20) and in accordance with the declaration of Helsinki.

2.2 Sample preparation

Human colon carcinoma specimens were formalin fixed (4% PFA for 24 h) and paraffin embedded using the following steps (3 h 60% ethanol, 3 h 75% ethanol, 3 h 96% ethanol, 3 h 100% ethanol, 3 h xylol, transferred and kept in warm paraffin prior embedding). A histology section of 2.5 μ m thickness was obtained and stained with hematoxylin and eosin (H&E) [25]. The blocks were then scanned at the SYRMEP beamline of the Italian synchrotron [26]. Following the micro-CT scan, specimens were either deparaffinized and split into pieces of approximately 5 \times 5 \times 3 mm size or cylindrical biopsies were taken using a skin punch biopsy needle (pfm medical, Germany) with a diameter of 6 mm. Both types of samples were then processed in the same way. The samples were deparaffinized using a descending ethanol series (4 h xylol (60°C), 59 h xylol, 2 \times 12 h 100% ethanol, 2 \times 4 h 96% ethanol, 2 \times 4 h 75% ethanol, 4 h 60% ethanol, 4 h 50% ethanol, 4 h H₂O), then embedded in 1% (pieces) or 0.7% (punches) Phytigel (MERCK, KGaA, Germany). The embedded specimen was washed in phosphate buffered saline (PBS). The clearing process was performed at room temperature while gently shaking the sample using the following steps: 4 h in 30% ethanol, 4 h in 50% ethanol, 16 h in 70% ethanol, 4 h in 90% ethanol, 4 h in 100% ethanol, and finally in benzyl alcohol/benzyl benzoate (BABB, ratio 1:3) until sufficient transparency was achieved, which typically required at least 5 days. After the clearing process the samples were kept in BABB and scanned again at the SYRMEP beamline. Figure 1 summarizes the different processing steps of the workflow, starting from acquiring histological slices and PBI scans from standard FFPE tissue block followed by optical clearing of deparaffinized tissue, to PBI imaging

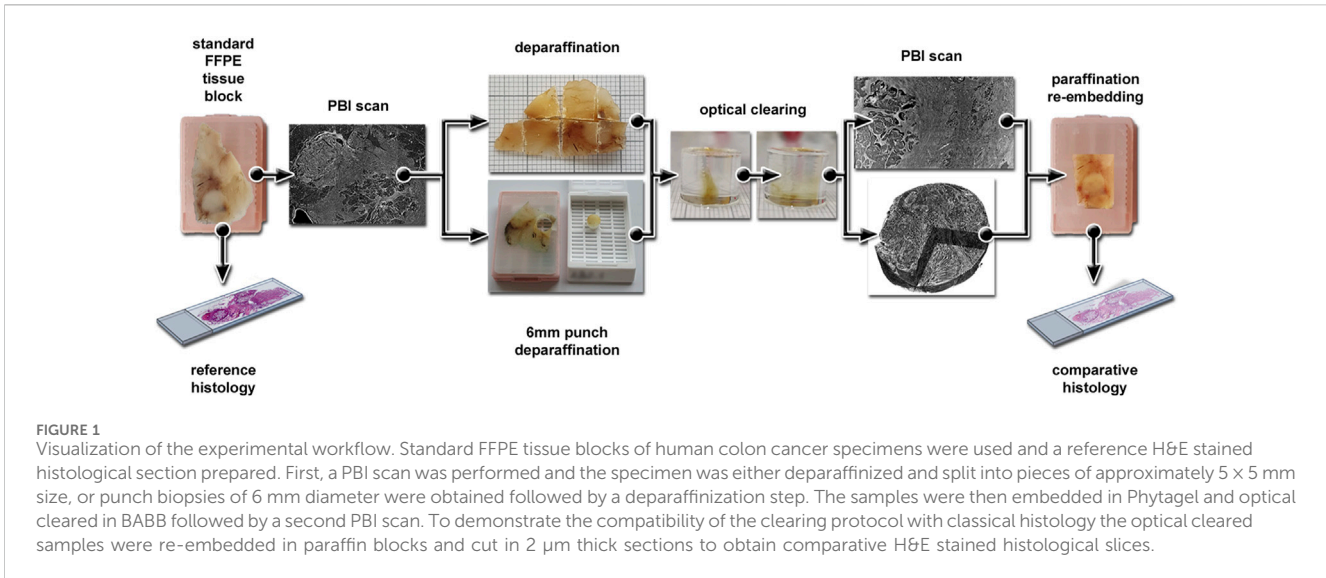


TABLE 1 Acquisition and image reconstruction parameters for the different specimen types.

	FFPE	BABB-pieces	BABB-punch
Sample-to-detector distance [cm]	15	50	50
Average energy [keV]	16.7	19.3	21.05
Projections	3,600	3,600	3,600
Mode	360° off-center	360° off-center	360° off-center
Exposure time	30 m	30 m	20 m
Total scanning time	108 s	108 s	180 s
Pixel size [μm]	1.9 μm	1.9 μm	2.0 μm
δ/β ratio	100	200	200

of the cleared samples and re-embedding of re-paraffinized tissue specimens.

2.3 Phase contrast microCT imaging and image reconstruction

All samples were scanned at the SYRMEP beamline of the Italian synchrotron Elettra using PBI with a white/pink beam setup. After the acquisition, single-distance phase retrieval (TIE-HOM [21]) was applied prior to 3D reconstruction with a standard filtered back projection algorithm. Parameters used are summarized in Table 1.

2.4 Parameters used for quantitative image quality assessment

For a comprehensive image quality assessment the following parameters such as contrast, noise and sharpness need to be calculated in parallel. Here we evaluated contrast-to-noise ratio (CNR) between homogeneous tissue regions and the embedding

material (paraffin or Phytigel respectively). The CNR is calculated using the following equation:

$$CNR = \frac{|\bar{g}_1 - \bar{g}_2|}{\sqrt{0.5 * (\sigma_1^2 + \sigma_2^2)}} \quad (1)$$

here, g_i and σ_i denoting the average grey value and the standard deviation of the grey values in a homogeneous regions of tissue and embedding material, respectively. We further calculated full width at half maximum (FWHM) of a differentiated line profile of tissue to embedding media interface to assess the edge sharpness.

2.5 Software

Phase retrieval and reconstruction of the synchrotron data was performed with SYRMEP Tomo Project (STP v1.5.2) [27]. CNR and FWHM were calculated using values extracted from micro-CT data using Fiji [28]. Statistical analysis and display of the result was done with *statannot* v0.2.3 [29] and *seaborn* v0.12.2 [30] using a Welch T-test with Bonferroni correction for multiple comparison (**** =

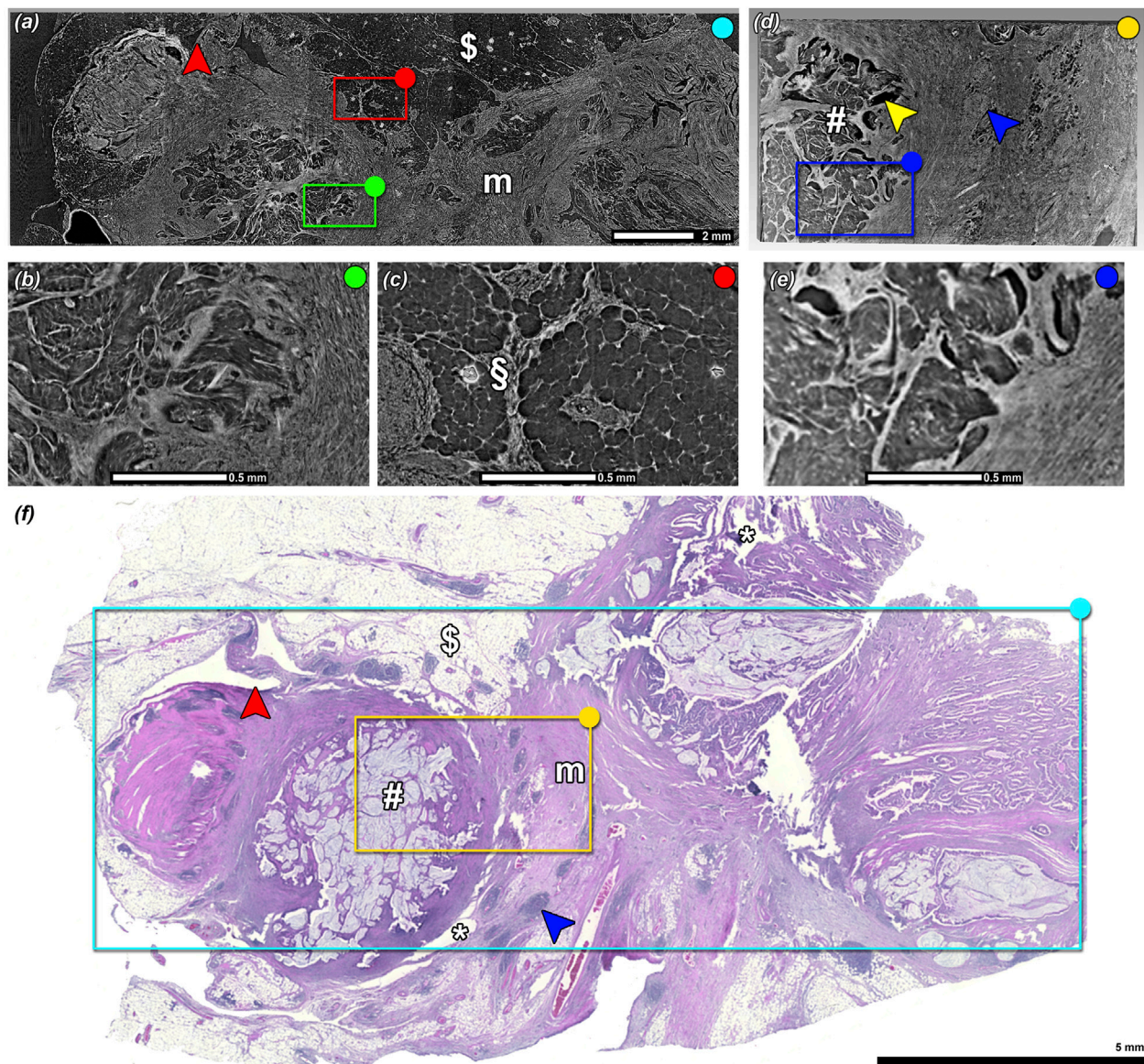


FIGURE 2

Comparison of PBI image between standard FFPE and BABB optical cleared tissue specimens. PBI scans obtained in FFPE condition (A) before optical clearing where (B) and (C) highlights the magnified regions of (A). (D) PBI scans after BABB optical clearing where (E) shows the magnified region of (D). (F) A-priori performed H&E stained histological section. (#) marks cancer derived mucin, (\$) fat tissue, (m) tumor induced fibrotic desmoplasia, (blue arrow head) lymph follicle. While the FFPE scan had some artifacts such as air bubbles (\$), note that none of those were found in the scan of the BABB cleared sample. The red arrow head indicates a region in which strong tissue deformation occurred in the histological sectioning process. The (*) marks regions that were ruptured. By visually assessing (B) and (E) the BABB sample data seems to provide comparable contrast and level of details found in the FFPE sample data.

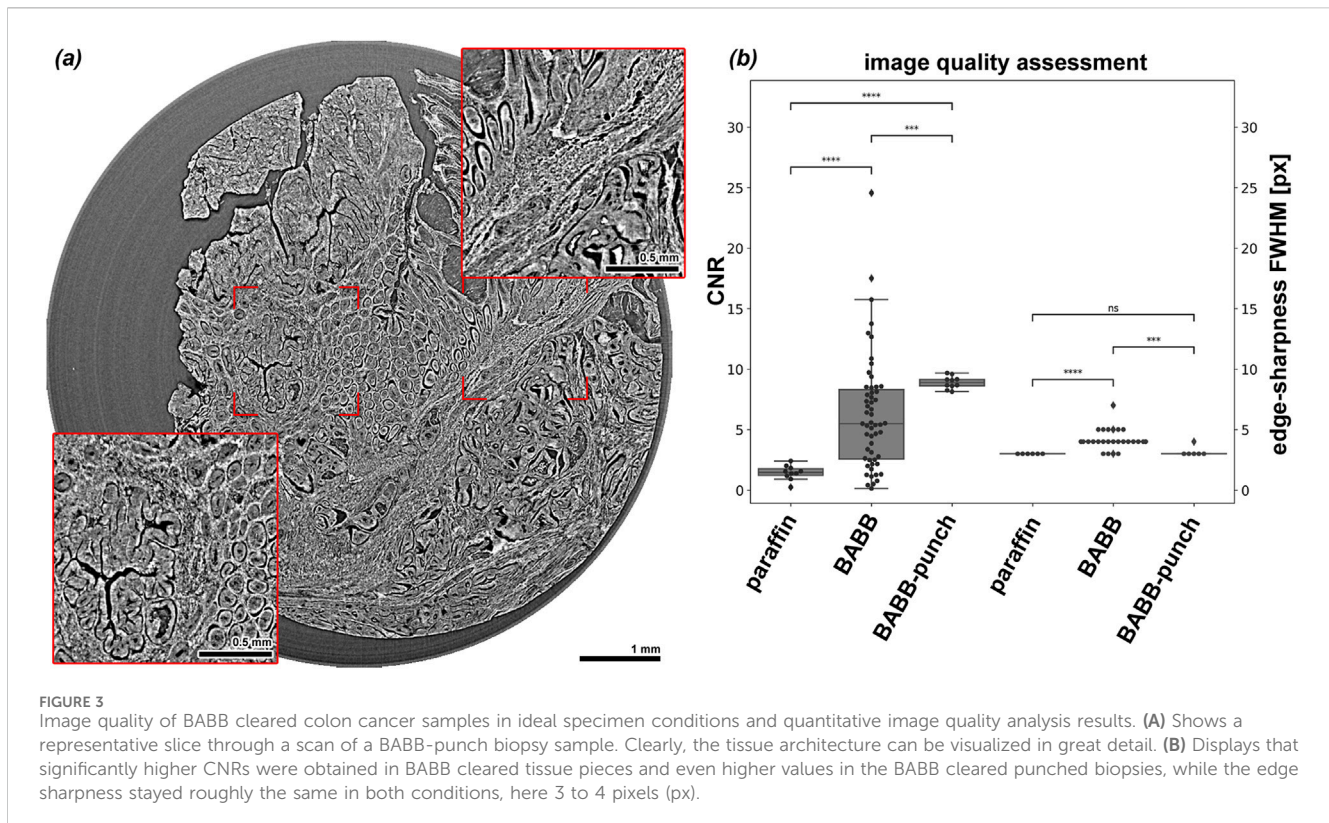
$p < 1e-4$, *** = $p < 1e-3$, ** = $p < 0.01$, * = $p < 0.05$ and ns = not significant).

3 Results and discussion

3.1 Visual image quality assessment

In Figure 2, a visual comparison of a specimen imaged in FFPE condition (Figure 2A, magnified regions Figures 2B, C) and after optical clearing (Figure 2D, magnified region Figure 2E) is presented with a corresponding histological slice taken prior PBI imaging

(Figure 2F). Five consecutive scans were performed to cover the core part of the FFPE specimen. The scanned region is indicated on the histological image (turquoise rectangle, Figure 2F). Note, that anatomical structures such as mucin rich areas (#), lymphatic tissue (blue arrow head), fat (\$), and muscle structures (m) can be identified. The magnified area in Figure 2B highlights the image quality that was achieved in a mucin rich region of the specimen scanned in FFPE condition where artifacts such as air inclusion are visible in Figure 2C (\$). One of the optical cleared tissue pieces (indicated in yellow in Figure 2F) of the same specimen is shown in Figure 2D. While a direct comparison of the grey values in 3D rendering of the PBI scans is difficult to achieve, the optical cleared



PBI data did not show any artifacts and the tissue structures and contrast appeared to be consistent with the PBI data set of the FFPE specimen as further indicated in the detailed 2D view (Figure 2E). The red arrow heads in Figure 2A and f indicate the deformation that occurred during the histological sectioning process of FFPE blocks, which also caused tissue ruptures, e.g., in areas marked with white asterisks (Figure 2F).

Micro-CT scans of the BABB optical cleared sample showed different tissue structures in details analogous to the FFPE tissue specimen. In addition, the BABB samples were free from apparent artifacts like air inclusions but showed minor shrinkage in the mucin rich regions (yellow arrow head, Figure 2D). The fact that all data were acquired with the same pixel size and obtained image quality appeared to be similar if not better in the BABB specimens, proving that indeed optical clearing is a viable alternative tissue preparation method for PBI setup. Although tissue embedded in other materials such as in agarose gel has been successfully scanned at synchrotron CT setups by different groups [5, 23], typically the large dose deposition bears the risk of melting the agarose gel which results in air bubble formation, especially at the tissue surface. Here using Pythagel instead of agarose gel in combination with optical clearing resulted in vastly transparent tissue specimens, thus the dose deposition was reduced and as a consequence no bubble formation was observed.

3.2 Quantitative image quality assessment

For quantitative image quality analysis, the CNR between tissue and embedding material was calculated. The evaluated noise in a

tissue region by measuring standard deviation of the gray values is constrained by the heterogeneity of the tissue structures and therefore overestimated the actual noise. Thus, the calculated CNR values underrepresented the real CNR of the data set. Figure 3A shows an example for a BABB cleared punch specimen. Clearly the complex architecture of the specimen can be resolved nearly at a cellular level. As shown in Figure 3B, a significant increase in CNR from FFPE (1.4 ± 0.6) to BAAB (6.2 ± 4.7) and a further increase in the punched BABB specimens (8.9 ± 0.5) was depicted. The comparison is slightly limited by the fact that single-distance phase retrieval applied to white/pink beam acquisition requires manual adjustment of the δ/β ratio to the specific sample conditions as well as that the specimens differed in their dimensions. However, increasing the δ/β ratio will result in an increased CNR (due to the low pass filtering effect of TIE-Hom) but that would in turn reduce the edge sharpness in FWHM. While the chosen δ/β ratio was higher in case of BABB cleared samples, the measured edge sharpness in FWHM between 3 and 4.2 pixel reveals that the increase in CNR was not attributed to an increasing low pass filtering.

The images of BABB cleared samples show a higher CNR and a comparable edge sharpness to the FFPE tissue. The punched samples with a diameter of 6 mm and precise cylindrical shape are ideal for PBI CT imaging at this resolution of $2 \mu\text{m}$ pixel size. In 360° -off-center scan mode using a detector with 2048×2048 pixel the maximum lateral field of view (FOV) is slightly below 8 mm (to achieve a meaningful overlap). As a consequence, scanning specimens with a diameter of 6 mm did not create local area scanning artifacts such as in the FFPE tissue blocks or in case of the BABB cleared tissue pieces. Therefore, the obtained increase of

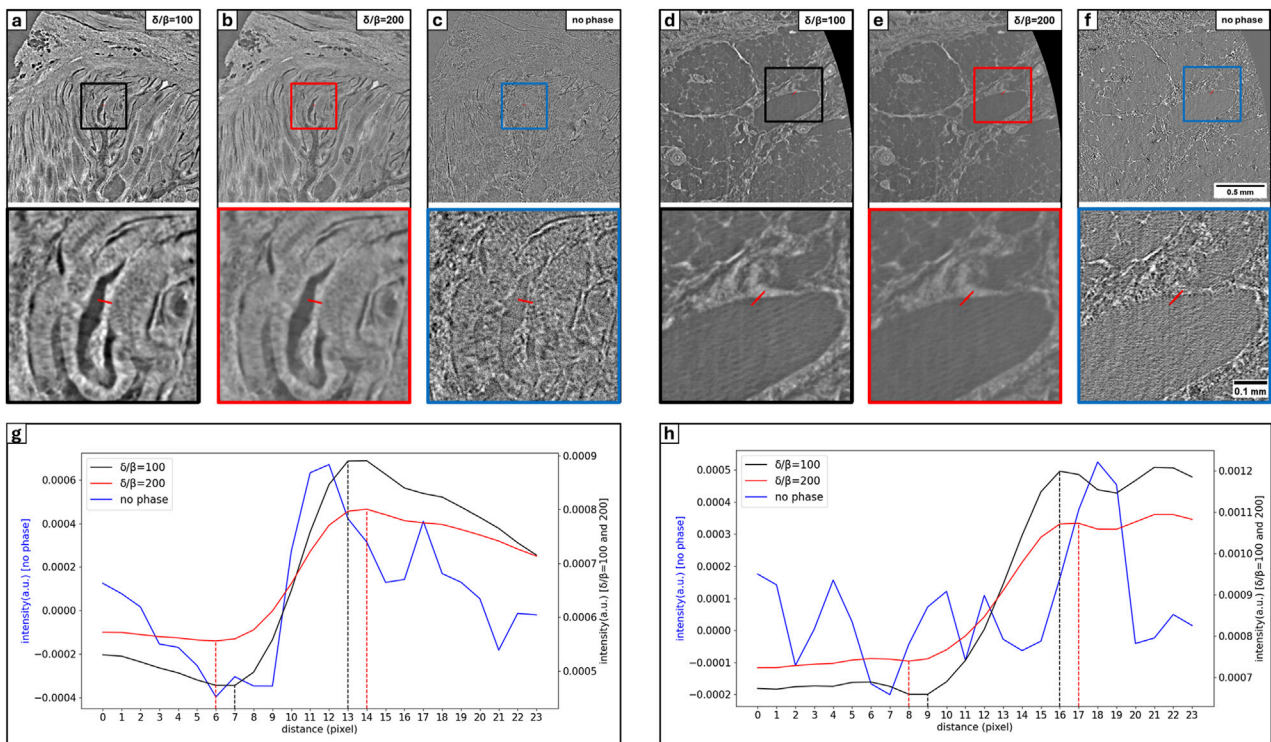


FIGURE 4

Comparison of intensity profile at the tissue interface with phytigel and paraffin for BABB punch and FFPE specimen respectively. Considered intensity profile (red line) is illustrated in (A–C) for the BABB punch and in (D–F) for the FFPE specimen with corresponding zoomed region (bottom rectangle). In both conditions specimens are reconstructed with $\delta/\beta = 100$ (A, D), 200 (B, E) and without phase retrieval (C, F). (G, H) show the resulted intensity profile plot at the indicated positions for BABB punch and FFPE specimen respectively. Intensity profile without phase retrieval in case of the BABB punch (blue in (G)) specimen clearly shows an edge with strong phase effect. Although $\delta/\beta = 100$ reduces strong negative and positive edge enhancement effects present in without phase retrieval profile and shows a smooth edge profile (black in (G)), $\delta/\beta = 200$ removes these effects (red in (G)) and was more adequate for the reconstruction. Unlike BABB punch FFPE specimen resulted a very noisy edge profile without phase retrieval (blue in (H)), however already with $\delta/\beta = 100$ edge profile (black in (H)) was almost free from negative and positive edge enhancement effects. In both cases the width of the edge shows an increase of 2 px (from 6 px to 8 px) for BABB punch and 1 px (7 px to 8 px) for FFPE specimen due to increase in δ/β indicates the effect of low pass filtering.

CNR and edge sharpness in the BABB-punch samples compared to the BABB cleared tissue pieces are most likely attributed to these geometrical conditions. Clearly, this analysis is limited by the fact that the chosen acquisition parameter had to be optimized for the different sample conditions and are therefore widely different. Nevertheless, it is safe to say that BABB cleared tissue performed at least as good as FFPE tissue in PBI and presents therefore a valid alternative to FFPE tissue preparation.

To further illustrate the differences in the obtained image quality as well as to motivate the choice of the different parameter, Figure 4 shows edge profiles in Figures 4A–4C of a BABB-punch and Figures 4D–4F of a FFPE specimen. The data was reconstructed with $\delta/\beta = 100$ (a and d), $\delta/\beta = 200$ (b and e) and without phase retrieval (c and f). The resulting profile plots at the indicated positions are shown in Figures 4G, H (blue = no phase retrieval, black = $\delta/\beta = 100$, red = $\delta/\beta = 200$). The BABB-punch specimen (g) shows a well defined edge without phase retrieval and strong phase effects indicated by the negative and positive edge enhancement. $\delta/\beta = 100$ results in a smooth edge profile but still shows remaining negative and positive edge enhancement. While with $\delta/\beta = 200$ the profile does not show these effects anymore and was therefore considered to be more adequate. Due to the low pass filtering effect the width of the edge

increased from 6 px (black, $\delta/\beta = 100$) to 8 px (red, $\delta/\beta = 200$). In case of the FFPE specimen the edge profile without phase retrieval is very noisy and $\delta/\beta = 100$ already nearly removed negative and positive edge enhancement completely. Here the width of the edge increases from 7 px (black, $\delta/\beta = 100$) to 8 px (red, $\delta/\beta = 200$). Thus based on the used parameter and condition the image quality of the BABB-punch specimen is comparable if not even better to the presented established FFPE tissue preparation and scanning protocol.

3.3 Compatibility for subsequent histological analysis

Following the imaging session and after removal of the Phytigel, the BABB optical cleared samples were re-embedded into paraffin. Next we validated if classical histology would still be possible to obtain comparable quality to routine paraffin sections. Figure 5 shows approximately the same region of the original H&E stained histological section (Figure 5A) in comparison to the PBI image (Figure 5B) and to H&E stained section of the re-embedded specimen (Figure 5C). A precise registration of the three data

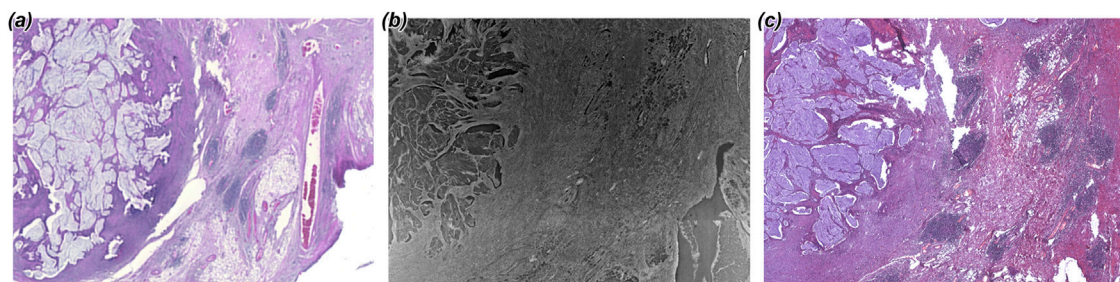


FIGURE 5

Comparison of H&E stained sections before and after optical clearing. (A) shows a region from the H&E stained histological slice obtained at the beginning of the workflow. (B) shows the PBI imaging result of the corresponding BABB cleared piece. (C) Presents a H&E stained slice after re-paraformaldehyde fixation and re-embedding of the same piece. While the colors are slightly different, no diminished quality of the histological section was found.

sets could not be achieved as changing the condition of the specimen led to small deformations. However, it can be seen in [Figure 5C](#) that the overall quality of the H&E staining is not diminished compared to the standard workflow using standard paraffin sections ([Figure 5A](#)). Thus, we propose that BABB optical clearing can be an applicable method for sample preparation for PBI alternative to FFPE tissue blocks even if the use of light sheet microscopy (LSM) is not intended, for which the clearing protocol was originally invented. However, the Phytigel embedded BABB cleared specimens cannot directly be cut with a classical microtome. Re-embedding in paraffin is required which led to comparable quality of histological images but may introduce tissue shrinkage and deformation rendering spatial integration of other imaging data as shown by [8] more challenging.

3.4 Applicability for other optical clearing methods

In this publication we focused solely on BABB clearing protocol. The contrast for specimen phase contrast CT seems way higher for dehydrated tissue than for fresh tissue or tissue in aqueous solutions as for instance demonstrated by Takeda et al. [31]. The good results with BABB are therefore most likely based on its ethanol content. Thus, it can be assumed that clearing protocols based on aqueous solutions will result in lower contrast in phase contrast CT. However, further tests are required to validate this assumption.

3.5 Summary

Here we present an alternative tissue sample preparation method and compared the image quality of PBI micro-CT scans of standard FFPE embedded with proposed BABB cleared human colon cancer specimens. The usage of the BABB optical clearing protocol yielded in an equivalent CNR and edge sharpness. In addition, typical challenges of FFPE tissue scans such as air inclusions and crack formation did not occur in the BABB specimens. We also show that optical clearing does not obstruct the possibility of subsequent classical histological analysis. Thus, we believe that BABB clearing not only is suitable for LSM but also presents a possible tissue preparation protocol for PBI virtual

histology approaches. In addition, deep learning methods where both LSM and micro-CT data are used to train models to predict clinical outcomes [32] by detecting morphological features in the tissue would benefit tremendously from the fact that the same specimens in the same conditions could be used in both methods.

Data availability statement

The raw data supporting the conclusions of this article will be made available by the authors, without undue reservation.

Ethics statement

The studies involving humans were approved by the local ethics committee of the University Medical Center Göttingen (permission number 24/4/20). The studies were conducted in accordance with the local legislation and institutional requirements. The human samples used in this study were acquired from gifted from another research group. Written informed consent for participation was not required from the participants or the participants' legal guardians/next of kin in accordance with the national legislation and institutional requirements.

Author contributions

MS: Conceptualization, Data curation, Formal Analysis, Investigation, Methodology, Software, Visualization, Writing—original draft, Writing—review and editing. AS: Data curation, Investigation, Methodology, Software, Writing—review and editing. LD: Data curation, Investigation, Methodology, Software, Visualization, Writing—review and editing. DP-L: Methodology, Writing—review and editing. JM-G: Funding acquisition, Methodology, Writing—review and editing. EL: Data curation, Investigation, Writing—review and editing. GT: Conceptualization, Methodology, Project administration, Resources, Supervision, Writing—review and editing. HB: Formal Analysis, Methodology, Writing—review and editing. FA: Conceptualization, Funding acquisition, Methodology, Project administration, Resources, Supervision, Writing—review and

editing, CD: Conceptualization, Data curation, Formal Analysis, Funding acquisition, Investigation, Methodology, Project administration, Software, Supervision, Visualization, Writing—original draft, Writing—review and editing.

Funding

The author(s) declare that financial support was received for the research, authorship, and/or publication of this article. The project was partially funded by the Niedersächsisches Ministerium für Wissenschaft und Kultur (MWK, ZN3822) and the EuroBioImaging (www.eurobioimaging.eu) initiative.

Acknowledgments

The authors thank Julia Fascher, Sabine Wolfgramm, Bettina Jeep, Sarah Garbode, Bärbel Heidrich and Regine Kruse for excellent technical assistance. We also like to express our gratitude to all members of the phase contrast CT imaging node of EuroBioImaging

References

- Albers J, Pacilé S, Markus MA, Wiart M, Vande Velde G, Tromba G, et al. X-ray-based 3d virtual histology—adding the next dimension to histological analysis. *Mol Imaging Biol* (2018) 20:732–41. doi:10.1007/s11307-018-1246-3
- Frohn J, Pinkert-Leetsch D, Missbach-Güntner J, Reichardt M, Osterhoff M, Alves F, et al. 3d virtual histology of human pancreatic tissue by multiscale phase-contrast x-ray tomography. *J Synchrotron Radiat* (2020) 27:1707–19. doi:10.1107/S1600577520011327
- Donato S, Arana Peña LM, Arfelli F, Brombal L, Colmo L, Longo R, et al. Integrating x-ray phase-contrast imaging and histology for comparative evaluation of breast tissue malignancies in virtual histology analysis. *Scientific Rep* (2024) 14:5831. doi:10.1038/s41598-024-56341-6
- Saccomano M, Albers J, Tromba G, Dobrovojević Radmilović M, Gajović S, Alves F, et al. Synchrotron inline phase contrast μ ct enables detailed virtual histology of embedded soft-tissue samples with and without staining. *J synchrotron Radiat* (2018) 25:1153–61. doi:10.1107/S1600577518005489
- Dullin C, Ufartes R, Larsson E, Martin S, Lazzarini M, Tromba G, et al. μ ct of *ex vivo* stained mouse hearts and embryos enables a precise match between 3d virtual histology, classical histology and immunohistochemistry. *PLoS one* (2017) 12:e0170597. doi:10.1371/journal.pone.0170597
- Albers J, Markus MA, Alves F, Dullin C. X-ray based virtual histology allows guided sectioning of heavy ion stained murine lungs for histological analysis. *Scientific Rep* (2018) 8:7712. doi:10.1038/s41598-018-26086-0
- Albers J, Svetlove A, Alves J, Kraupner A, di Lillo F, Markus MA, et al. Elastic transformation of histological slices allows precise co-registration with microct data sets for a refined virtual histology approach. *Scientific Rep* (2021) 11:10846. doi:10.1038/s41598-021-89841-w
- D'Amico L, Svetlove A, Longo E, Meyer R, Senigaglia B, Saccomano G, et al. Characterization of transient and progressive pulmonary fibrosis by spatially correlated phase contrast microct, classical histopathology and atomic force microscopy. *Comput Biol Med* (2024) 169:107947. doi:10.1016/j.compbimed.2024.107947
- Khan A, Markus AM, Svetlove A, Hülsmann S, Alves F, Dullin C (2023). Monitoring the response to nintedanib treatment in a mouse model of lung fibrosis using longitudinal x-ray based lung function measurement. *Research Squ*. doi:10.21203/rs.3.rs-2780852/v1
- de Oliveira CS, González AT, Hedtke T, Kürbitz T, Heilmann A, Schmelzer CE, et al. Direct three-dimensional imaging for morphological analysis of electrospun fibers with laboratory-based zernike x-ray phase-contrast computed tomography. *Mater Sci Eng C* (2020) 115:111045. doi:10.1016/j.msec.2020.111045
- Eckermann M, Frohn J, Reichardt M, Osterhoff M, Sprung M, Westermeier F, et al. 3d virtual pathohistology of lung tissue from covid-19 patients based on phase contrast x-ray tomography. *Elife* (2020) 9:e60408. doi:10.7554/elifelife.60408

at the Italian synchrotron including the engineering department and the scientific computing group.

Conflict of interest

Authors LD, EL, GT and CD were employed by Elettra Synchrotron SCpa Trieste.

The remaining authors declare that the research was conducted in the absence of any commercial or financial relationships that could be construed as a potential conflict of interest.

Publisher's note

All claims expressed in this article are solely those of the authors and do not necessarily represent those of their affiliated organizations, or those of the publisher, the editors and the reviewers. Any product that may be evaluated in this article, or claim that may be made by its manufacturer, is not guaranteed or endorsed by the publisher.

- Taba ST, Baran P, Lewis S, Heard R, Pacile S, Nesterets YI, et al. Toward improving breast cancer imaging: radiological assessment of propagation-based phase-contrast ct technology. *Acad Radiol* (2019) 26:e79–e89. doi:10.1016/j.acra.2018.07.008
- Horng A, Brun E, Mittone A, Gasilov S, Weber L, Geith T, et al. Cartilage and soft tissue imaging using x-rays: propagation-based phase-contrast computed tomography of the human knee in comparison with clinical imaging techniques and histology. *Invest Radiol* (2014) 49:627–34. doi:10.1097/rli.0000000000000063
- Peña LA, Donato S, Bonazza D, Brombal L, Martellani F, Arfelli F, et al. Multiscale x-ray phase-contrast tomography: from breast ct to micro-ct for virtual histology. *Physica Med* (2023) 112:102640. doi:10.1016/j.ejmp.2023.102640
- Riedel M, Hammel JU, Moosmann J, Beckmann F, Schwarzenberg F, Schuetz P, et al. Quantitative phase-contrast x-ray micro ct for visualization of mouse lymph nodes. *Dev X-Ray Tomography XIV (Spie)* (2022) 12242:224–30. doi:10.1117/12.2631184
- Barbone GE, Bravin A, Mittone A, Grosu S, Ricke J, Cavaletti G, et al. High-spatial-resolution three-dimensional imaging of human spinal cord and column anatomy with postmortem x-ray phase-contrast micro-ct. *Radiology* (2021) 298:135–46. doi:10.1148/radiol.2020201622
- Eckermann M, Van der Meer F, Cloetens P, Ruhwedel T, Möbius W, Stadelmann C, et al. Three-dimensional virtual histology of the cerebral cortex based on phase-contrast x-ray tomography. *Biomed Opt express* (2021) 12:7582–98. doi:10.1364/boe.434885
- Cercos-Pita J-L, Fardin L, Leclerc H, Maury B, Perchiazzi G, Bravin A, et al. Lung tissue biomechanics imaged with synchrotron phase contrast microtomography in live rats. *Scientific Rep* (2022) 12:5056. doi:10.1038/s41598-022-09052-9
- Pinkert-Leetsch D, Frohn J, Ströbel P, Alves F, Salditt T, Missbach-Guentner J. Three-dimensional analysis of human pancreatic cancer specimens by phase-contrast based x-ray tomography—the next dimension of diagnosis. *Cancer Imaging* (2023) 23:43. doi:10.1186/s40644-023-00559-6
- Langer M, Cloetens P, Guigay JP, Valton S, Peyrin F. Quantitative evaluation of phase retrieval algorithms in propagation based phase tomography. In: *2007 4th IEEE international symposium on biomedical imaging: from Nano to Macro (IEEE)* (2007). p. 552–5.
- Paganin D, Mayo SC, Gureyev TE, Miller PR, Wilkins SW. Simultaneous phase and amplitude extraction from a single defocused image of a homogeneous object. *J Microsc* (2002) 206:33–40. doi:10.1046/j.1365-2818.2002.01010.x
- Beltran MA, Paganin DM, Uesugi K, Kitchen MJ. 2d and 3d x-ray phase retrieval of multi-material objects using a single defocus distance. *Opt Express* (2010) 18:6423–36. doi:10.1364/oe.18.006423
- Strotton MC, Bodey AJ, Wanelik K, Darrow MC, Medina E, Hobbs C, et al. Optimising complementary soft tissue synchrotron x-ray microtomography for

- reversibly-stained central nervous system samples. *Scientific Rep* (2018) 8:12017. doi:10.1038/s41598-018-30520-8
24. Maglio M, Salamanna F, Brogini S, Borsari V, Pagani S, Nicoli Aldini N, et al. Histological, histomorphometrical, and biomechanical studies of bone-implanted medical devices: hard resin embedding. *Biomed Res Int* (2020) 2020:1–13. doi:10.1155/2020/1804630
25. Cardiff RD, Miller CH, Munn RJ. Manual hematoxylin and eosin staining of mouse tissue sections. *Cold Spring Harbor Protoc* (2014) 2014:pdb.prot073411. doi:10.1101/pdb.prot073411
26. Dullin C, di Lillo F, Svetlove A, Albers J, Wagner W, Markus A, et al. Multiscale biomedical imaging at the symep beamline of elettra-closing the gap between preclinical research and patient applications. *Phys Open* (2021) 6:100050. doi:10.1016/j.physo.2020.100050
27. Brun F, Pacilè S, Accardo A, Kourousias G, Dreossi D, Mancini L, et al. Enhanced and flexible software tools for x-ray computed tomography at the Italian synchrotron radiation facility elettra. *Fundamenta Informaticae* (2015) 141:233–43. doi:10.3233/fi-2015-1273
28. Schindelin J, Arganda-Carreras I, Frise E, Kaynig V, Longair M, Pietzsch T, et al. Fiji: an open-source platform for biological-image analysis. *Nat Methods* (2012) 9:676–82. doi:10.1038/nmeth.2019
29. Charlier F, Weber M, Izak D, Harkin E, Magnus M, Lalli J, et al. *Statannotations* (2022). doi:10.5281/zenodo.7213391
30. Waskom ML. seaborn: statistical data visualization. *J Open Source Softw* (2021) 6:3021. doi:10.21105/joss.03021
31. Takeda T, Kunii T, Sirai R, Ohizumi T, Maruyama H, Hyodo K, et al. Ethanol fixed brain imaging by phase-contrast x-ray technique. *J Phys Conf Ser* (2013) 425:022004. doi:10.1088/1742-6596/425/2/022004
32. Song AH, Williams M, Williamson DF, Chow SS, Jaume G, Gao G, et al. Analysis of 3d pathology samples using weakly supervised ai. *Cell* (2024) 187:2502–20.e17. doi:10.1016/j.cell.2024.03.035